Zeno–anti-Zeno crossover dynamics in a spin–boson system

2010 J. Phys. A: Math. Theor. 43 155301

(http://iopscience.iop.org/1751-8121/43/15/155301)

IOP PUBLISHING JOURNAL OF PHYSICS A: MATHEMATICAL AND THEORETICAL

J. Phys. A: Math. Theor. **43** (2010) 155301 (14pp) doi:10.1088/1751-8113/43/15/155301

Zeno–anti-Zeno crossover dynamics in a spin–boson system

A Thilagam

Applied Centre for Structural and Synchrotron Studies, University of South Australia, Adelaide 5095, Australia

E-mail: thilaphys@gmail.com

Received 2 September 2009, in final form 9 February 2010
Published 25 March 2010
Online at stacks.iop.org/JPhysA/43/155301

Abstract

We examine the critical system parameters which affect the quantum Zeno–anti-Zeno transition in a spin–boson system by applying the notion of correlated Zeno subspaces beyond the qubit system to its decayed part represented by a collective reservoir of oscillators. We also examine the effect of coherent control via a periodic sequence of dynamical decoupling pulses *prior* to projective measurement. Our results show that depending on the system bias and measurement time interval of the spin–boson model, coherent control via periodic dynamical decoupling pulses eliminates the Zeno–anti-Zeno transition behavior. We extend the calculations to examine the entanglement dynamics of two initially entangled qubits coupled to independent reservoirs with varying configuration and subjected to frequent measurements. In a multipartite system, in which one or more qubit–reservoir system can undergo the Zeno–anti-Zeno transition, we show that the effects of measurements made in a one qubit–reservoir subsystem can reverberate noticeably throughout a whole array of N pairs of qubit–reservoir subsystems.

PACS numbers: 03.65.Xp, 03.65.Yz, 03.65.Ud, 03.67.Mn

(Some figures in this article are in colour only in the electronic version)

1. Introduction

The quantum Zeno effect (QZE) describes the retarded time evolution of a quantum state subjected to frequent measurements [1–3]. In the limiting case of continuous measurement, the time evolution of the state is expected to come to a standstill. The opposite effect which leads to enhancement in time evolution is known as anti-Zeno effect (AZE) and has been observed to be much more ubiquitous than the Zeno effect [4, 5]. In unstable systems, the occurrence of both QZE and AZE depends on critical parameters, such as measurement frequencies and environmental noise [6, 7]. In recent years, experimental demonstrations of

the QZE [8, 9] have been driven by interest in practical applications such as the reduction of decoherence in quantum computing systems [10–12].

The spin–boson is a very well known model where a two-level system is coupled to a reservoir of harmonic oscillators and is useful in quantifying salient aspects of dissipative dynamics of many quantum systems [13, 14]. Factors such as spectral density, bias and temperature which determine decoherence [15, 16] are also seen to play a critical role in the fine interplay of the QZE and AZE in the spin–boson model [17]. In this work, we analyze the dependence of the Zeno–anti-Zeno transition point on critical parameters of the spin–boson model. We specifically chose this model as the features of the Zeno–anti-Zeno transition have recently been shown to be highly prominent in bosonic spin-bath systems [17].

It is important to note the two seemingly different criteria used to specify the quantum Zeno–anti-Zeno transition point in the literature. In the first approach by Facchi *et al* [18], an effective decay rate $\gamma(\tau)$ measured at $t = \tau$ is compared to the natural decay rate γ_0 which does not involve measurement. A $\gamma(\tau)$ smaller than γ_0 is attributed to the Zeno effect while $\gamma(\tau)$ larger than γ_0 is attributed to the anti–Zeno effect. The transition point occurs at the intersection of the effective decay rate at a specific time known as jump time [18]. In an alternate scheme proposed by Kofman and Kurizki [4, 5], the emphasis is on the rate of change of effective decay rate with respect to frequency of measurement unlike a direct comparison with the natural decay rate.

Kofman and Kurizki's formalism involves the convolution of two functions: a measurement function and a reservoir coupling function dependent on the spectral density of states of the reservoir [5]. The occurrence of the QZE or AZE is easily explained [5] by changes in the overlap between the two functions as τ is varied. The QZE (AZE) occurs when the overlap of functions decreases (increases) with the decrease in τ. At the critical crossover point, there is no net change in the overlap function, the decay rate stops momentarily and the criterion for the Zeno–anti-Zeno crossover is given by $\partial\gamma/\partial\tau = 0$. A similar relation was obtained by Pati *et al* [19] who showed the relation between the survival probability and speed of transportation of a system point on the projective Hilbert space. Thus, measurements made with a time interval less than a critical time duration (transition point) slows down decay whereas those made using a time interval larger than the critical time interval speed up the decay of a quantum state. Kofman and Kurizki's approach is convenient in cases where the existence of a jump time (which can be very small in many unstable systems) is difficult to determine. Kofman and Kurizki's approach also provides a neat explanation for anti–Zeno effects which exist wherever there is a large detuning between the peaks of the measurement function and reservoir coupling function. This latter point will be illustrated for the spin–boson model in section 3.1.

We next study the effects of dynamical decoupling schemes [20–22] on the Zeno–anti-Zeno transition regime. During the process of dynamical decoupling, a quantum system is subjected to several successive (periodic, random or recursive) strong ultrafast pulses which offset any undesirable decoherence due to an environment represented by the surrounding reservoir. The interaction between the qubit spin and boson reservoir is generally assumed to be linear in the amplitude of the boson field. This approach is based on the time reversal of the decoherence process in a short-time scale comparable to the reservoir correlation time. Efforts to enhance this scheme, which *does not* involve collapse of the wavefunction which otherwise occurs during measurement, have grown rapidly due to its potential applications in quantum information processing. Recent works [23, 24] on the dynamic control of decay via 2π pulses have shown that the decay can in fact be accelerated depending on reservoir and pulsing properties. In our work here, we specifically examine the effect of coherent control via periodic dynamical decoupling pulses [21] on the occurrence of a Zeno–anti-Zeno crossover.

Finally, we extend results obtained in the first section to examine the conditions under which Zeno or anti-Zeno effects present in several qubit–reservoir systems influence the overall entanglement of multipartite systems. We also consider entanglement sudden death (birth) which is the finite-time loss (gain) of quantum correlation due to independent reservoirs coupled to the two qubits with regard to the Zeno–anti-Zeno transition [25, 26]. The strength of coupling between qubit and reservoir, number of subsystems, measurement procedures as well as the initial configuration of qubit–resevoir systems are shown to be critical factors in the entanglement properties of multipartite systems. Thus, the effect of a measurement process in one qubit–reservoir subsystem is felt throughout the whole array of qubit–reservoir subsystems, and we demonstrate this quantitatively via use of the Meyer–Wallach measure for general N pairs of qubit–reservoir systems.

2. Zeno–anti-Zeno transition in spin–boson systems

Various approximation schemes [27–29] are commonly used to study spin–boson problems involving both strong and weak coupling to the reservoir. A common approach involves examining the dynamics of the density matrix contained in the Liouville equation

$$\frac{\partial \rho}{\partial t} = -\mathrm{i}[\widehat{H}_{\mathrm{T}}, \rho(t)], \tag{1}$$

where the total Hamiltonian of a two-level qubit system $\widehat{H}_{\mathrm{T}} = \widehat{H}_{\mathrm{qb}} + \widehat{H}_{\mathrm{os}} + \widehat{H}_{\mathrm{qb-os}}$. $\widehat{H}_{\mathrm{qb}}$ of the two-level qubit is of the form

$$\widehat{H}_{\mathrm{qb}} = \hbar \left(\frac{\Delta\Omega}{2} \sigma_z + \Delta \sigma_x \right), \tag{2}$$

where the Pauli matrices are expressed in terms of the two possible states $(|0\rangle, |1\rangle)$, $\sigma_x = |0\rangle\langle 1| + |1\rangle\langle 0|$ and $\sigma_z = |1\rangle\langle 1| - |0\rangle\langle 0|$. $\Delta\Omega$ is the biasing energy while Δ is the tunneling amplitude. Each qubit is coupled to its own reservoir of harmonic oscillators $\widehat{H}_{\mathrm{os}} = \sum_{\mathbf{q}} \hbar\omega_{\mathbf{q}} b^{\dagger}_{\mathbf{q}} b_{\mathbf{q}}$ where $b^{\dagger}_{\mathbf{q}}$ and $b_{\mathbf{q}}$ are the respective creation and annihilation operators of the quantum oscillator with the wave vector $\mathbf{q}$. We consider the qubit–oscillator interaction Hamiltonian to be linear in terms of oscillator creation and annihilation operators:

$$\widehat{H}_{\mathrm{qb-os}} = \sum_{\mathbf{q}} \lambda_{\mathbf{q}} \left(b^{\dagger}_{\mathbf{q}} + b_{\mathbf{q}} \right) \sigma_z, \tag{3}$$

where $\lambda_{\mathbf{q}}$ is the coupling between the qubit and the environment and is characterized by the spectral density function, $J(\omega) = \sum_{\mathbf{q}} \lambda^2_{\mathbf{q}} \delta(\omega - \omega_{\mathbf{q}})$. Here, we consider the density functions to be of the ohmic form $J(\omega) = 2\pi\eta\omega\, \mathrm{e}^{-\frac{\omega}{\omega_c}}$ where η is the dimensionless reservoir coupling function. ω_c is the reservoir cutoff frequency and is generally assumed to be the maximum allowed frequency. For simplicity in analysis of the entanglement dynamics, we exclude the measuring device from the total Hamiltonian $\widehat{H}_{\mathrm{T}} = \widehat{H}_{\mathrm{qb}} + \widehat{H}_{\mathrm{os}} + \widehat{H}_{\mathrm{qb-os}}$. The reservoir therefore constitutes a part of the dynamical system that is monitored by the measuring device which serves only as a projection operator that disrupts the normal evolution of the Hamiltonian $\widehat{H}_{\mathrm{T}}$. This treatment is consistent with the viewpoint [30] that the presence of a macroscopic apparatus is *not* a prerequisite to the measurement process.

At $t = 0$, the reservoirs associated with the two qubits are uncorrelated. Each qubit decays to oscillator states in the reservoir when measurements are made, making a transition from its excited state $|1\rangle_{\mathrm{q}}$ to the ground state $|0\rangle_{\mathrm{q}}$. We consider an initial state of the qubit with

its corresponding reservoir in the vacuum state, existing in equilibrium at temperature $T = 0$ K:

$$|\phi_i\rangle = |1\rangle_{\rm q} \otimes \prod_{k=1}^{N'} |0_k\rangle_{\rm r} = |1\rangle_{\rm q} \otimes |\mathbf{0}\rangle_{\rm r}, \tag{4}$$

where $|\mathbf{0}\rangle_{\rm r}$ implies that all N' wavevector modes of the reservoir are unoccupied in the initial state. $|\phi_i\rangle$ then undergoes the following mode of decay:

$$|\phi_i\rangle \longrightarrow u(t)\ |1\rangle_{\rm q}|\mathbf{0}\rangle_{\rm r} + v(t)\ |0\rangle_{\rm q}|\mathbf{1}\rangle_{\rm r}. \tag{5}$$

In order to keep the problem tractable, we consider that $|\mathbf{1}\rangle_{\rm r}$ denotes a collective state of the reservoir as follows:

$$|\mathbf{1}\rangle_{\rm r} = \frac{1}{v(t)} \sum_n \lambda_{\{n\}}(t)|\{n\}\rangle, \tag{6}$$

where $\{n\}$ denotes an occupation scheme in which there are n_i oscillators with the wavevector $k = i$ in the reservoir, and we define the state $|\{n\}\rangle$ as

$$|\{n\}\rangle = |n_0, n_1, n_2, \ldots, n_i, \ldots, n_{N'}\rangle. \tag{7}$$

In the collective reservoir state, oscillators can be present at all allowed modes, including simultaneous excitation of several bosonic states. At non-zero temperatures, the reservoir state is a Boltzmann weighted average over all possible permutations of the occupation scheme $\{n\}$. In the absence of any form of coupling between the qubit and reservoir oscillator, transitions between the states $|\{n\}\rangle$ and $|\{n'\}\rangle$ where $n \neq n'$ are *not allowed* due to orthogonal properties of oscillator functions. This is a critical property as it confines the evolution of the initial reservoir state $|\mathbf{0}\rangle_{\rm r}$ to its quantum Zeno subspace, as long as the qubit remains in its initial state $|1\rangle_{\rm q}$. The definition of the collective state of the reservoir in equation (7) obviously gives rise to entanglement between the qubit and reservoir state. We next describe in detail the important concept of quantum zeno subspaces.

2.1. Quantum Zeno subspaces

Following [1, 31], we use the von Neumann projection operator $\mathcal{P}$ to formulate measurement procedures in the Hilbert space $\mathcal{H}$ of a quantum system, S. The initial density matrix ρ_0 of the system S is constrained within $\mathcal{H}_\mathcal{P}$ as $\rho_0 = \mathcal{P}\rho_0\mathcal{P}$, $\mathrm{Tr}[\rho_0\mathcal{P}] = 1$. In the absence of any measurement, the state evolves as $\rho(t) = U(t)\rho_0 U^\dagger(t)$ where $U(t) = \exp(-\mathrm{i}H^\star t)$, and $H^\star$ is a time-independent Hamiltonian. The probability that the system remains within $\mathcal{H}_\mathcal{P}$ is given by $P(t) = \mathrm{Tr}\,(U(t)\rho_0 U^\dagger(t)\mathcal{P})$. In the event of measurement at time τ, the density matrix $\rho(\tau)$ becomes $\rho(\tau) = \frac{1}{P(\tau)}\mathcal{P}U(\tau)\rho_0 U^\dagger(\tau)\mathcal{P}$. The survival probability in $\mathcal{H}_\mathcal{P}$ becomes $P(\tau) = \mathrm{Tr}\,(V(\tau)\rho_0 V^\dagger(\tau))$ where $V(\tau) \equiv \mathcal{P}U(\tau)\mathcal{P}$. For the case of measurements at time intervals $\tau = t/N$, the survival probability is given by

$$P^{(N)}(t) = \mathrm{Tr}\left(V_N(t)\rho_0 V_N^\dagger(t)\right), \qquad V_N(t) = \left[V\left(\frac{t}{N}\right)\right]^N. \tag{8}$$

At very large N, no transitions allowed outside $\mathcal{H}_\mathcal{P}$ occur and $P^{(N)}(t) \to 1$, the culmination of the mathematical formulation of the Zeno effect.

The functions $u(t)$ and $v(t)$ in equation (5) satisfy the relation $u(t)^2 + v(t)^2 = 1$. We identify the square of the function $u(t)$ with the survival probability of the qubit associated with N measurements performed at regular intervals τ via the relation

$$P(t) = u(t)^2 = \exp(-N\Delta^2\tau^2/4) \tag{9}$$

with time $t = N\tau$. In the extreme limit $\tau \to 0, u(t) \to 1$ and the decay into oscillator states is totally inhibited. Equations (8) and (9) embody the powerful effect of a measurement process in itself, where a system monitored to determine whether it remains in a particular state resists making transitions to alternate states. This idea has been studied using an adiabatic theorem [31] in which different outcomes are eliminated and the system evolves as a group of exclusive quantum Zeno subspaces within the total Hilbert space. The initial state remains in a particular invariant subspace which ensures that the survival probability remains unchanged from its value of one. The time evolution within the projected Zeno subspace gives rise to quantum Zeno effects [1] as mathematically formulated in equation (8). The time invariance property associated with the Zeno effect may have implications for equivalent processes which lead to the existence of decoherence free subspaces widely discussed in the literature [32].

The interaction Hamiltonian term $\widehat{H}_{\text{qb–os}}$ in equation (3) gives rise to intriguing effects of the measurement process by governing the dynamical evolution of quantum systems. This term has a decomposing effect on the total Hilbert space which is partitioned into orthogonal quantum Zeno subspaces [31] mentioned earlier. The qubit system is then constrained into predestined paths within each invariant subspace. Likewise we invoke the notion of Zeno subspaces beyond the qubit system to its decayed part represented by the collective reservoir. We note that corresponding to the invariant subspace occupied by the initial qubit state $|1\rangle_{\text{q}}$, there exists an invariant Zeno subspace associated with the initial reservoir state $|\mathbf{0}\rangle_{\text{r}}$ in which all modes are unoccupied. Importantly this Zeno subspace remains orthogonal to subspaces where second-order processes exist, by virtue of the othorgonality. Such processes give rise to exchanges between oscillators and overall changes in the ensemble configuration of oscillators in the reservoir. This implies that when the qubit is measured in the initial state $|1\rangle_{\text{q}}$ at $t = \tau$, the reservoir also remains in its initial state $|\mathbf{0}\rangle_{\text{r}}$ by virtue of the orthogonality of oscillator functions in the defined reservoir state in equation (7). This ensures that the invariance of $P_0(\tau)$ at equidistant measurement intervals remains intact. A thorough mathematical analysis of the joint evolution of the qubit and reservoir system and the time evolution within the correlated subspace can be examined using the idea of entangled Zeno subspaces, however, it is beyond the scope of work here.

It is easy to identify an effective relaxation rate for the two-level qubit that is reliable at short times, $\gamma(\tau) = N(\Delta/2)^2\tau$. The decay of a quantum state interacting with a reservoir is almost zero at the beginning of the decay process as is well known in the QZE. In the cases of intermediate measurement time intervals, the decay of the quantum state may be accelerated as is the case in anti-Zeno effect (AZE). These effects are however not evident in the short time range associated with equation (9), in which the fine interplay between the measurement procedure and the reservoir coupling function is not fully incorporated. Therefore, in the next section, we utilize the numerical scheme introduced by Kofman and Kurizky [4, 5] to estimate $\gamma(\tau)$ and to reveal the interesting quantum Zeno–anti-Zeno transition effects inherent in a spin–boson system. This scheme will be crucial in studying the entanglement dynamics of qubit–reservoir systems subjected to different modes of measurements characterized by τ. It is important to note that only the time duration (instead of frequency) of measurement is altered and its effect analyzed in figures obtained in this work.

3. Effective decay rate using Kofman and Kurizky's formalism

The effective decay rate for small values of τ is evaluated as a convolution of two functions [4, 5]:

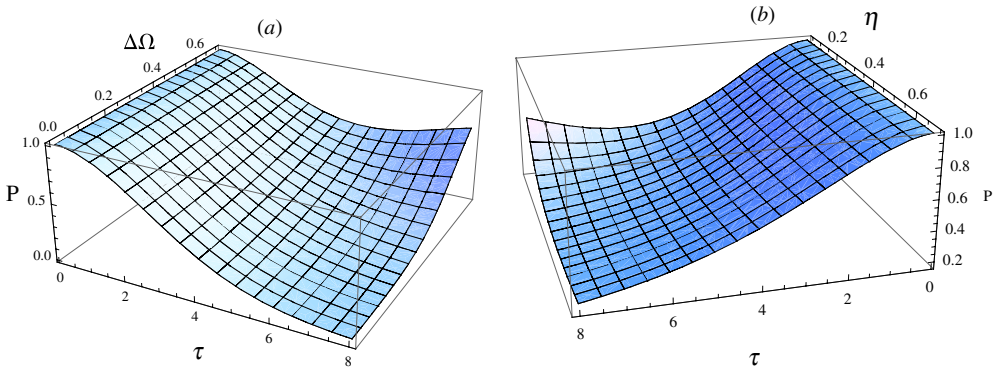

Figure 1. (*a*) Survival probability $P(\tau)$ as a function of the time duration τ and the bias $\Delta\Omega$ after the first measurement at $T = 0$ K, $\Delta = 0.6$, $\eta = 0.05$ and $\omega_c = 1$. (*b*) Survival probability $P(\tau)$ as a function of the time interval τ and the reservoir coupling function η at $T = 0$ K, $\Delta = 0.6$, $\omega_c = 1$ and bias $\Delta\Omega = 0.65$.

$$\gamma(\tau) = 2\left(\frac{\Delta}{2}\right)^2 \int_0^\infty \mathrm{d}\omega\, K(\omega) F_\tau(\omega - \Delta\Omega), \tag{10}$$

where the function $F_\tau(\omega - \Delta\Omega) = \frac{\tau}{2\pi}\,\mathrm{sinc}^2\left[\frac{(\omega-\Delta\Omega)\tau}{2}\right]$ and is associated with measurements at intervals of τ. The reservoir coupling function $K(\omega)$ is evaluated using

$$K(\omega) = \int_0^\infty \mathrm{e}^{\mathrm{i}\omega t} \cos[\Delta\Omega + G_1(t)]\, \mathrm{e}^{-G_2(t)}\, \mathrm{d}t, \tag{11}$$

where

$$\begin{aligned} G_1(t) &= \int_0^\infty \mathrm{d}\omega \frac{J(\omega)}{\omega^2} \sin\omega t \\ G_2(t) &= \int_0^\infty \mathrm{d}\omega \frac{J(\omega)}{\omega^2} \coth\left[\frac{\beta\omega}{2}\right](1 - \cos\omega t) \end{aligned} \tag{12}$$

where $\beta = \frac{1}{k_B T}$ and T is the lattice temperature. Using explicit expressions for $G_1(t)$ and $G_2(t)$ given in [13, 14] for an ohmic $J(\omega)$, it can be shown that $K(\omega)$ is strongly dependent on the reservoir coupling function η and the exponential cutoff frequency ω_c, and of the form $K(\omega) \approx \left(\frac{\omega}{\omega_c}\right)^{2\eta-1} \exp(-\omega/\omega_c)$. Figure 1(*a*) shows the numerical results of the survival probability $P(t) = \exp(-\gamma(\tau)t)$ after the first measurement ($N = 1$) at zero temperature, tunneling amplitude $\Delta = 0.6$, reservoir coupling function $\eta = 0.05$ and $\omega_c = 1$. We note that an increase in the frequency of measurement corresponds to a decrease in time duration between measurements. Figure 1(*a*) shows that the crossover from the QZE to AZE becomes increasingly pronounced as τ is increased, provided the spin–boson system experiences weak spin–boson coupling η as illustrated in figure 1(*b*). It is interesting to note that Zeno to anti-Zeno features are revealed even with the first measurement. Hence, higher biasing energies $\Delta\Omega$ and lower η increase the probability of the Zeno–anti-Zeno transition, which occurs at $\partial P(t)/\partial\tau = 0$. Due to the highly prominent Zeno–anti-Zeno transition for a weakly coupled system ($\eta \sim = 0.05$), we focus on the entanglement properties of the weakly coupled system in section 5 associated with measurement procedures. It is to be noted that the theory established so far is applicable at non-zero temperatures; however, we have specifically chosen $T = 0$ K for ease of numerical computation for all figures in this work.

A natural decay rate γ_0 at $T = 0$ K can be obtained by noting $F_\tau(\omega) \to 1$ as $\tau \to \infty$

$$\gamma_0 = \frac{\Delta^2}{2} \frac{\Delta\Omega^{2\eta-1}}{\Gamma(2\eta)} \exp(-\Delta\Omega) \tag{13}$$

where we have used $\omega_c = 1$. For the bias range $0.1 \leqslant \Delta\Omega \leqslant 0.8$, $\Delta = 0.6$ and $\eta = 0.05$ (same parameters as used in figure 1), we obtain very small $\gamma_n(\tau) \leqslant 0.1$ that hardly compares with the rich Zeno dynamics revealed via Kofman and Kurizky's formalism. This demonstrates that $\gamma_n(\tau)$ is not a suitable reference to predict the Zeno–anti-Zeno dynamics in the spin–boson model considered here.

3.1. Effect of dynamical decoupling on the Zeno–anti-Zeno transition

Here, we consider a two-level qubit system to be subjected to M successive optical π pulses of very short duration before projective measurement is performed. The first π-pulse rotates the qubit state vector through an angle π about the x-axis, while the second pulse inverts the state vector back to its initial state. Under the action of two π pulses, the reversal of time evolution of the qubit system is achieved, assuming decay times in the non-Markovian dynamics regime [20]. The Hamiltonian representing the dynamic decoupling pulses is written as [21, 33, 34]

$$\hat{H}_{\rm pul} = \sum_{n=1}^{M} V_n(t)\, \mathrm{e}^{\mathrm{i}\frac{\Delta\Omega}{2}t\sigma_z}\, \sigma_x\, \mathrm{e}^{-\mathrm{i}\frac{\Delta\Omega}{2}t\sigma_z}, \tag{14}$$

where a periodic sequence of M equidistant ideal π-pulses are applied at times $t_M = M\Delta t$ and Δt denotes the inter-pulse separation time. In the presence of the dynamic decoupling pulses, the spectral function $F_\tau(\omega)$ in equation (10) modifies as

$$F'_\tau(\omega) = F_\tau(\omega) \tan^2 \frac{\omega\Delta t}{2}. \tag{15}$$

We set $\tau = 2M\Delta t + \delta t$ where δt is a very short time lapse to ensure that the last control pulse precedes measurement. The dynamic decoupling pulse term $\tan^2 \frac{\omega\Delta t}{2}$ in equation (15) suppresses decoherence [21] at low frequencies $\omega_u = 2M\pi/(\tau - \delta t) \approx 2M\pi/\tau$ and enhances decoherence at higher frequencies $\omega_u \approx 3M\pi/\tau$ depending on the cutoff frequency and the form of spectral density function, $J(\omega)$ [33]. Figure 2 shows numerical results of the decay rate $\gamma(\tau)$ evaluated using equation (10) with a modified measurement function $F'_\tau(\omega)$ (equation (15)) at $T = 0$ K, $M = 1$ or $M = 3$ and for two values of the bias $\Delta\Omega = 0.35, 0.5$. At $M = 1$, the two upper frequency limits of $\omega_u = 2M\pi/\tau$ and $\omega_u = 3M\pi/\tau$ are used during numerical computations. We note that $M = 1$ denotes the application of two π-pulses before the instant measurement is performed. The low cutoff frequency $\omega_u = 2M\pi/\tau$ yields lower decay rates as expected. We note that the M π-pulses are equally spaced out; hence, an increase of M implies a corresponding decrease in the inter-pulse separation time Δt. This results in detuning of central frequencies of the coupling function $K(\omega)$ and measurement function $F'_\tau(\omega)$, giving rise to changes in the spectral overlap between the two functions. Figure 3 clearly illustrates the decrease of the overlap function O as M is increased from one to two at weak bias $\Delta\Omega = 0.35$. This explains the notable suppression of decay at higher M values. At a higher $\Delta\Omega = 0.5$, $F'_\tau(\omega)$ experiences increased oscillatory peaks which results in shifts such that the overlap of the two functions increases at larger τ, contrary to the situation at low bias.

It is to be noted that there remains the possibility of the Hamiltonian in equation (14) leading to the formation of a nontrivial subspace in itself, thus presenting with a complicated structure the analysis carried out in figure 2. We believe that the existence of subspaces associated with equation (14) may give rise to interesting effects that may be verified via experimental work.

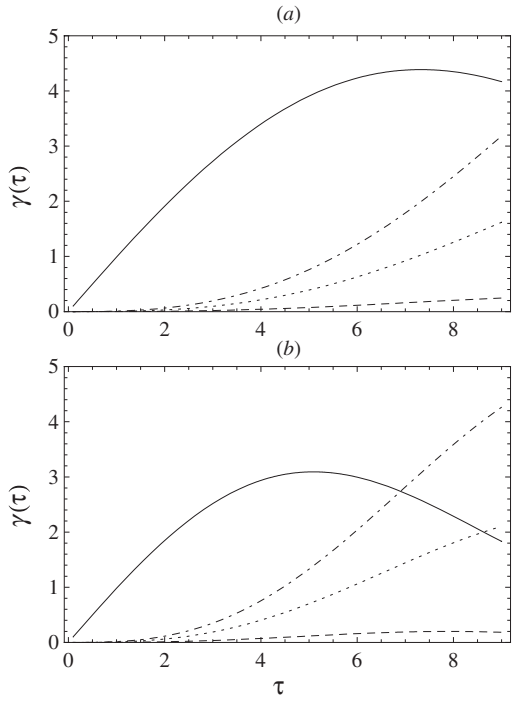

Figure 2. (*a*) $\gamma(\tau)$ evaluated using equations (10) and (15) at $T = 0$ K, $M = 1$, upper frequency cutoff limit $\omega_u = 3M\pi/\tau$ (dot-dashed), $\omega_u = 2M\pi/\tau$ (dotted) and $M = 3$, $\omega_u = 3M\pi/\tau$ (dashed). $\eta = 0.1$, $\omega_c = 1$ and bias $\Delta\Omega = 0.35$ apply for all curves. The solid line denotes evaluation of $\gamma(\tau)$ in the *absence* of dynamical decoupling pulses. (*b*) Same parameters as in (*a*) above except that the bias is increased, $\Delta\Omega = 0.5$.

4. Concurrence as a measure of counteracting Zeno–anti-Zeno effects

We now consider the joint evolution of a pair of two-level qubit systems in uncorrelated reservoirs subjected to distinct measurement procedures with differing values of the time interval τ. We first consider the following initial state:

$$|\Phi\rangle_0 = [a|0\rangle_{q1}|0\rangle_{q2} + b|1\rangle_{q1}|1\rangle_{q2}]|0\rangle_{r1}|0\rangle_{r2}, \tag{16}$$

where $i = 1, 2$ denote the two qubit–reservoir system's associated function $u_i(t)$ (see equation (5)). Each function $u_i(t)$ corresponds to the measurement parameter τ_i. a, b are real coefficients and satisfy $a^2 + b^2 = 1$. The state $|\Phi\rangle_0$ evolves as a multipartite state influenced by the real coefficients a and b, similar to the process considered in our earlier work [35]. Using the conversion rule given in equation (5), we obtain for instance the following evolution for terms associated with coefficient b:

$$\begin{aligned} b|1\rangle_{q1}|1\rangle_{q2}|0\rangle_{r1}|0\rangle_{r2} \rightarrow\ & b[u_1(t)|1\rangle_{q1}|0\rangle_{r1} + v_1(t)|0\rangle_{q1}|1\rangle_{r1}] \\ & \times [u_2(t)|1\rangle_{q2}|0\rangle_{r2} + v_2(t)|0\rangle_{q2}|1\rangle_{r2}]. \end{aligned} \tag{17}$$

Using both terms of (16) and tracing out the reservoir states, we obtain a time-dependent qubit–qubit reduced density matrix in the basis $(|0\,0\rangle, |0\,1\rangle|1\,0\rangle|1\,1\rangle)$:

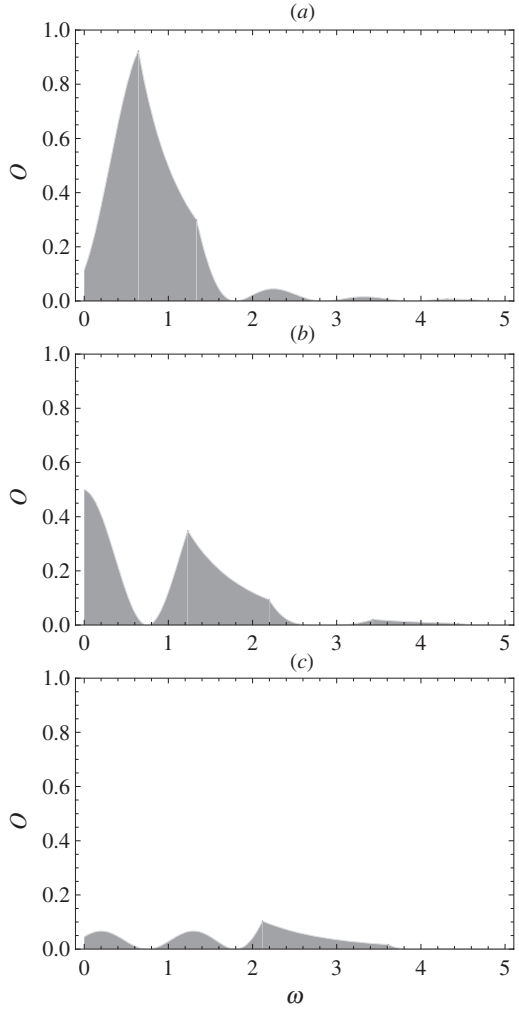

Figure 3. (*a*) Overlap O of spectral functions $K(\omega)$ and $F'_\tau(\omega)$ for $T = 0$ K, $\eta = 0.2$, bias $\Delta\Omega = 0.35$, $\tau = 6$ and $\omega_c = 1$. Three cases with (*a*) maximum overlap in the absence of dynamical decoupling pulses, dynamical decoupling pulses applied with (*b*) $M = 1$ and (*c*) $M = 2$.

$$\rho_{\mathrm{q1,q2}}(t) = \begin{pmatrix} f_1(t) & 0 & 0 & f_5(t) \\ 0 & f_2(t) & 0 & 0 \\ 0 & 0 & f_3(t) & 0 \\ f_5(t) & 0 & 0 & f_4(t) \end{pmatrix} \tag{18}$$

where for $t \geqslant 0$, the matrix elements evolve as

$$\begin{aligned} f_1(t) &= a^2 + b^2\, v_1(t)^2\, v_2(t)^2, & f_2(t) &= b^2\, v_1(t)^2\, u_2(t)^2, \\ f_3(t) &= b^2\, u_1(t)^2\, v_2(t)^2, & f_4(t) &= b^2\, u_1(t)^2\, u_2(t)^2, \\ f_5(t) &= a\, b\, u_1(t)\, u_2(t). \end{aligned} \tag{19}$$

The reservoir–reservoir reduced density matrix $\rho_{\mathrm{r1,r2}}$ is obtained by tracing out qubit states:

$$\rho_{\mathrm{r1,r2}}(t) = \begin{pmatrix} g_1(t) & 0 & 0 & g_5(t) \\ 0 & g_2(t) & 0 & 0 \\ 0 & 0 & g_3(t) & 0 \\ g_5(t) & 0 & 0 & g_4(t) \end{pmatrix} \tag{20}$$

where the functions g_i are obtained from f_i via the swap $u_i \leftrightarrow v_i$. Thus, the reduced bipartite density matrices $\rho_{\mathrm{q1,q2}}$ and $\rho_{\mathrm{r1,r2}}$ possess forms which are complementary to each other. These matrices also have simple forms with the well-known X-state structure which preserves its form during evolution. In order to study the QZE and AZE on the bipartite entanglements, we evaluate the well-known property of concurrence [36] for the appropriate density matrix using $\mathcal{C}(t) = \max\{0, \sqrt{\lambda_1} - \sqrt{\lambda_2} - \sqrt{\lambda_3} - \sqrt{\lambda_4}\}$ where λ_i are eigenvalues in decreasing order of the Hermitian matrix $\widetilde{\rho} = \rho(\sigma_y^1 \otimes \sigma_y^2)\rho^*(\sigma_y^1 \otimes \sigma_y^2)$ where σ_y belongs to the set of Pauli matrices. ρ^* denotes the complex conjugation of ρ in the standard basis equation (18). We obtain the following concurrence for the bipartite partition of the two qubits as well as their reservoir counterparts for $c = d = 0$:

$$\begin{aligned} \mathcal{C}_{\mathrm{q1,q2}}(t) &= 2b\,\mathrm{e}^{-\frac{1}{2}(\gamma_1+\gamma_2)t}\left[a - b(1-\mathrm{e}^{-\gamma_1 t})^{\frac{1}{2}}(1-\mathrm{e}^{-\gamma_2 t})^{\frac{1}{2}}\right] \\ \mathcal{C}_{\mathrm{r1,r2}}(t) &= 2b(1-\mathrm{e}^{-\gamma_1 t})^{\frac{1}{2}}(1-\mathrm{e}^{-\gamma_2 t})^{\frac{1}{2}}\left[a - b\,\mathrm{e}^{-\frac{1}{2}(\gamma_1+\gamma_2)t}\right]. \end{aligned} \tag{21}$$

For $\gamma_1 = \gamma_2 = \gamma$, we obtain simple expressions for the critical measurement time duration which leads to entanglement sudden death (ESD) and sudden birth (ESB) of qubit–qubit and reservoir–reservoir bipartite interactions respectively:

$$t_{\mathrm{q1,q2}} = -\frac{1}{\gamma(\tau)} \log\left[1 - \frac{a}{b}\right], \tag{22}$$

$$t_{\mathrm{r1,r2}} = -\frac{1}{\gamma(\tau)} \log\left[\frac{a}{b}\right]. \tag{23}$$

The effect of combining subsystems with different bias $\Delta\Omega_2$ and subjected to measurement with varying time interval τ on the qubit–qubit concurrence $\mathcal{C}_{\mathrm{q1,q2}}(\tau)$ and reservoir–reservoir concurrence $\mathcal{C}_{\mathrm{r1,r2}}(\tau)$ is shown in figure 4. The figure is plotted using numerical results of the survival probability $P(\tau) = \exp(-\gamma(\tau)\tau)$ at a tunneling amplitude $\Delta = 0.6$, $\eta = 0.05$, $\omega_c = 1$, $N = 1$, initial state amplitude $a = \frac{1}{\sqrt{5}}$ and fixed first subsystem bias of $\Delta\Omega_1 = 0.7$. These results show that the entanglement properties between two qubits can be altered by an appropriate choice of the time interval τ and system parameters such as the bias $\Delta\Omega$. Figure 4(*b*) also shows that the birth and subsequent death of the reservoir–reservoir bipartite interaction become prominent at higher values of the bias $\Delta\Omega_2$ associated with the second subsystem. At $b = 2a$ (i.e. $a = \sqrt{1/5}$), the death events associated with the bipartite partition matrix $\rho_{\mathrm{q1,q2}}$ coincide with birth events for its counterpart partition matrix $\rho_{\mathrm{r1,r2}}$. The notable change in entanglement dynamics with an initial state amplitude $a = \sqrt{1/\mu}$ where μ is varied is illustrated in figures 5(*a*) and (*b*). At high enough bias values for both subsystems and a selected range of μ, the Zeno–anti-Zeno transition gives rise to rebirth in qubit–qubit concurrence $\mathcal{C}_{\mathrm{q1,q2}}(\tau)$. We also note that the reservoir–reservoir concurrence $\mathcal{C}_{\mathrm{r1,r2}}(\tau)$ is short-lived for $6 < \mu < 8$, but becomes dominant at lower μ values. Next, we consider a second class of the initial state of the following form:

$$|\Phi\rangle_0 = [c|0\rangle_{\mathrm{ex1}}|1\rangle_{\mathrm{ex2}} + d|1\rangle_{\mathrm{ex1}}|0\rangle_{\mathrm{ex2}}]|0\rangle_{\mathrm{r1}}|0\rangle_{\mathrm{r2}}, \tag{24}$$

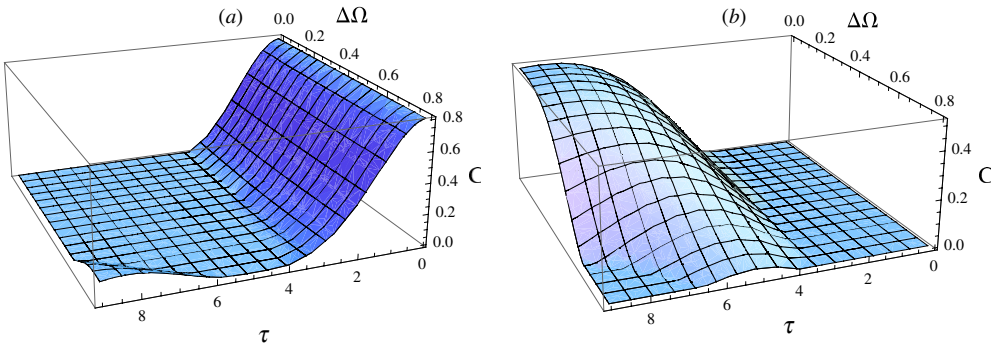

Figure 4. (*a*) Three-dimensional plot of the two-qubit concurrence $\mathcal{C}_{\mathrm{q1,q2}}(\tau)$ as a function of the measuring parameter τ and subsystem bias $\Delta\Omega_2$ for the initial state of equation (16) with $a = \sqrt{1/5}$ and fixed first subsystem bias of $\Delta\Omega_1 = 0.7$. We have taken a tunneling amplitude $\Delta = 0.6$, $\eta = 0.05$, $\omega_c = 1$ and $N = 1$. (*b*) Two-reservoir concurrence $\mathcal{C}_{\mathrm{r1,r2}}(\tau)$ as a function of the measuring parameter τ and subsystem bias $\Delta\Omega_2$. All other parameters remain the same as in (*a*).

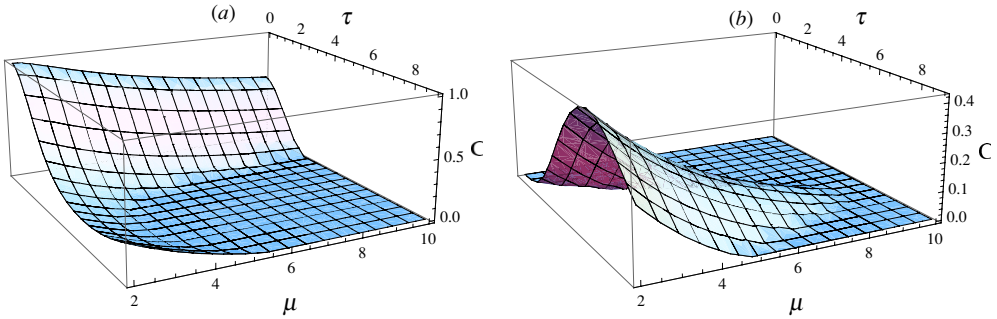

Figure 5. (*a*) Two-qubit concurrence $\mathcal{C}_{\mathrm{q1,q2}}(\tau)$ as a function of the measuring parameter τ and initial amplitude parameter μ ($a = \sqrt{1/\mu}$ in equation (16)) at subsystem bias $\Delta\Omega_1 = \Delta\Omega_2 = 0.6$, tunneling amplitude $\Delta = 0.6$, $\eta = 0.05$, $\omega_c = 1$ and $N = 1$. (*b*) Two-reservoir concurrence $\mathcal{C}_{\mathrm{r1,r2}}(\tau)$ as a function of the measuring parameter τ and initial amplitude parameter μ. All other parameters remain the same as in (*a*).

where $i = 1, 2$ denote the two qubit–reservoir systems with associated functions $u_i(t)$. As in the case of equation (19), we trace out the reservoir states to obtain a time-dependent exciton–exciton reduced density matrix

$$\rho_{\mathrm{q1,q2}}(t) = \begin{pmatrix} f_1(t) & 0 & 0 & 0 \\ 0 & f_2(t) & f_4(t) & 0 \\ 0 & f_4(t) & f_3(t) & 0 \\ 0 & 0 & 0 & 0 \end{pmatrix} \tag{25}$$

where for $t \geqslant 0$, the matrix elements evolve as

$$\begin{aligned} f_1(t) &= c^2\, v_2(t)^2 + d^2\, v_1(t)^2, \\ f_2(t) &= c^2\, u_2(t)^2, \qquad f_3(t) = d^2\, u_1(t)^2, \\ f_4(t) &= cd\, u_1(t) u_2(t). \end{aligned} \tag{26}$$

The concurrence for the bipartite partition of the two qubits as well as their reservoir counterparts can be evaluated respectively as $\mathcal{C}_{\mathrm{q1,q2}}(t) = 2cd\,\mathrm{e}^{-\frac{1}{2}(\gamma_1+\gamma_2)}$ and $\mathcal{C}_{\mathrm{r1,r2}}(t) = 2cd(1-\mathrm{e}^{-\gamma_1 t})^{\frac{1}{2}}(1-\mathrm{e}^{-\gamma_2 t})^{\frac{1}{2}}$. For this case, we note that the qubit–qubit bipartite interactions are immune from sudden death events due to measurement procedures. Due to normalization and positivity conditions associated with the X-state structured matrix, the partitions associated with $c = d = 0$ and $a = b = 0$ are not satisfied simultaneously.

5. Meyer–Wallach measure of N pairs of the qubit–reservoir system

In this section, we extend the analysis of two pairs of the qubit–reservoir system to a general N pair by considering the Meyer–Wallach (MW) measure with a generalized function u_i for the pair of qubit–reservoir system in equation (16). This monotone measure was defined by Meyer and Wallach [37] as a single scalar measure of pure state entanglement for the three- and four-qubit cases:

$$Q = \frac{1}{n}\sum_{k=1}^{n} 2\big(1 - \mathrm{Tr}\big[\rho_k^2\big]\big), \tag{27}$$

where ρ_k is the reduced density matrix of the kth qubit obtained after tracing out all the remaining qubits. While the MW measure has drawbacks in that it is unable to distinguish states which are fully inseparable from states which are separable into states of some set of subsystems, we will utilize it as a crude quantity to analyze qualitative features associated with the Zeno–anti-Zeno crossover in spin–bath systems.

For $c = d = 0$, the simple forms for the one-qubit reduced density matrices allow us to obtain an explicit expression of the MW measure of N pairs of qubit–reservoir systems:

$$Q = 2a^2b^2 + 4b^2u^2v^2 \tag{28}$$

where we have assumed that $u_i = u$ for all the N pairs. The maximum $Q = 1$ is obtained for $a = 0, b = 1$ with $u_1 = u_2 = \frac{1}{\sqrt{2}}$. For the case of N pairs of equivalent qubit–reservoir systems for which $u_i = u_1$ and S pairs of equivalent qubit–reservoir systems for which $u_i = u_2$, $(u_1 \neq u_2)$ we obtain

$$Q = \frac{2N}{N+S}(a^2b^2 + 2b^2{u_1}^2{v_1}^2) + \frac{2S}{N+S}(a^2b^2 + 2b^2{u_2}^2{v_2}^2). \tag{29}$$

Figure 6 shows the change of the Meyer–Wallach measure Q with τ for various combinations of N and S and for two values of the initial state amplitude, $a = \frac{1}{\sqrt{2}}$ and $a = \frac{1}{\sqrt{16}}$. A highly entangled system is obtained when all subsystems are in unison operating at the same bias $\Delta\Omega_1 = 0.7$ and linked by a small amplitude $a = \sqrt{1/16}$. The amplitude a gives a measure of correlation between the subsystems in their ground states. The survival probability $P(t)$ is high in each subsystem for such a configuration; hence, Q reaches high values for the range $4 \leqslant \tau \leqslant 6$. Increasing b (by decreasing a) accentuates the differences between the various combinations of subsystems and increases the influence of a measuring tool, as is expected of a strongly correlated multipartite system. Subsystems with larger bias ($\Delta\Omega_1 = 0.7$) undergo higher survival probability with projective measurement, and hence larger Q values are obtained in multipartite systems with high N values. The influence of the measuring tool from subsystems with zero bias will be increasingly felt as S is increased. Lower Q values are obtained when the system configuration is altered to one where S becomes high. We emphasize the inherent difficulties associated with the recursive nature of measurement procedures neglected in the simple model adopted here; the measurement of one system influences a second system being measured, which in turn affects the first system and vice

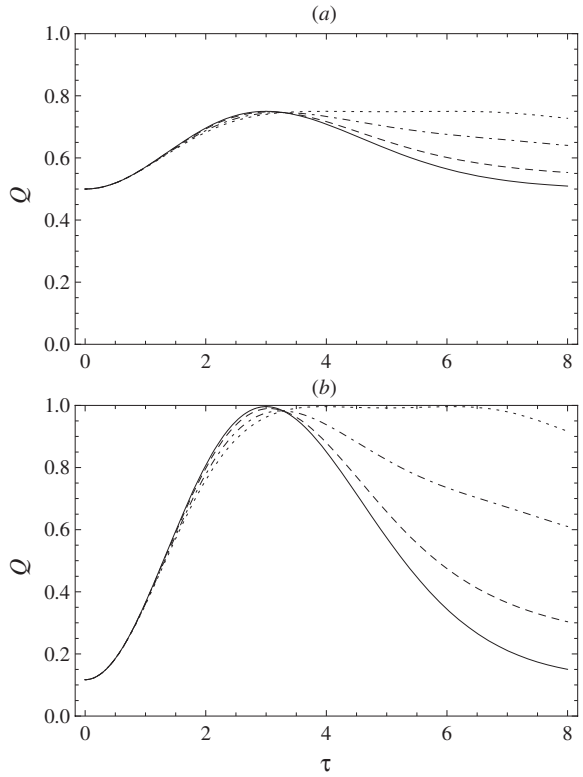

Figure 6. (*a*) Meyer–Wallach measure Q (equation (29)) as a function of the measuring parameter τ, for N pairs of qubit–reservoir systems for which $u_i = u_1$ and for S pairs for which $u_i = u_2$. Q is obtained using $a = \sqrt{1/2}$, $u_1(t) = \exp(-\gamma_1 t/2)$ and $u_2(t) = \exp(-\gamma_2 t/2)$. γ_1 (γ_2) is evaluated using the bias $\Delta\Omega_1 = 0.7$ ($\Delta\Omega_2 = 0$) via equation (10). We have used $\Delta = 0.6$, $\eta = 0.05$, $\omega_c = 1$ and $T = 0$ K for both u_1 and u_2. $N = 0, S = 5$ (solid lines), $N = 1, S = 4$ (dashed), $N = 3, S = 2$ (dot-dashed), $N = 5, S = 0$ (dotted). (*b*) Same parameters as above but using $a = \sqrt{1/16}$ instead.

versa. Even incorporating such intricacies, we can conclude with the gross result of our model, that is, the effects of a measurement tool in one or more qubit–reservoir subsystems can influence the overall entanglement of the array of qubit–reservoir subsystems.

It is important to note that the results obtained so far are generic to any two-level qubit system undergoing quantum state conversion and not specific to the spin–boson model undergoing exchanges with a reservoir of harmonic oscillators as considered here.

6. Conclusions

We have examined the dependence of the quantum Zeno–anti-Zeno transition point on the critical parameters of the spin–boson model. We have also studied the effect of coherent control via dynamical decoupling schemes *prior* to the measurement process on the characteristics of the Zeno–anti-Zeno transition. We find that coherent control via periodic dynamical decoupling pulses eliminates the Zeno–anti-Zeno transition behavior, depending on the bias $\Delta\Omega$ and measurement time interval τ of the spin–boson sub-systems. We also show that the

strength of coupling between qubit and reservoir, number of qubit–reservoir subsystems, measurement procedures, as well as the initial configuration of qubit–reservoir systems, play critical roles in entanglement properties of multipartite systems undergoing projective measurements. Finally, our results may have implications in studies involving the existence of entangled Zeno subspaces in multipartite systems in which one or more subsystems are subjected to measurement.

References

[1] Misra B and Sudarshan E C G 1977 *J. Math. Phys.* **18** 758
[2] Itano W M, Heinzen D J, Bollinger J J and Wineland D J 1990 *Phys. Rev.* A **41** 2295
[3] Facchi P and Pascazio S 2008 *J. Phys. A: Math. Theor.* **41** 493001
[4] Kofman A G and Kurizky G 2000 *Nature* **405** 546
[5] Kofman A G and Kurizky G 1996 *Phys. Rev.* A **54** 3750
[6] Fischer M C, Gutiérrez-Medina B and Raizen M G 2001 *Phys. Rev. Lett.* **87** 040402
[7] Maniscalco S, Piilo J and Suominen S A 2006 *Phys. Rev. Lett.* **97** 130402
[8] Zurek E W 2006 *Phys. Rev. Lett.* **97** 260402
[9] Nakanishi T, Yamane K and Kitano M 2001 *Phys. Rev.* A **65** 013404
[10] Zurek W H 1984 *Phys. Rev. Lett.* **53** 391
[11] Facchi P, Tasaki S, Pascazio S, Nakazato H, Tokuse A and Lidar D A 2005 *Phys. Rev.* A **71** 022302
[12] Maniscalco S, Francica F, Zaffino R L, Lo Gullo N and Plastina F 2008 *Phys. Rev. Lett.* **100** 090503
[13] Leggett A J, Chakravarty S, Dorsey A T, Fisher M P A, Grag A and Zwerger W 1995 *Rev. Mod. Phys.* **59** 1
[14] Weiss U 1999 *Quantum Dissipative Systems* (Singapore: World Scientific)
[15] Thilagam A and Lohe M A 2008 *J. Phys.: Condens. Matter* **20** 315205
[16] Thilagam A 2010 *Phys. Rev.* A **81** 032309
[17] Segal D and Reichman D R 2007 *Phys. Rev.* A **76** 012109
[18] Facchi P, Nakazato H and Pascazio S 2001 *Phys. Rev. Lett.* **86** 2699
[19] Pati A K and Lawande L V 1998 *Phys. Rev.* A **58** 831
[20] Ban M 1998 *J. Mod. Opt.* **45** 2315
[21] Viola L and Lloyd S 1998 *Phys. Rev.* A **58** 2733
[22] Uhrig G S 2007 *Phys. Rev. Lett.* **98** 100504
[23] Agarwal G S, Scully M O and Walther H 2001 *Phys. Rev.* A **63** 044101
[24] Zhang W and Zhuang J 2009 *Phys. Rev.* A **79** 012310
[25] Ting Yu and Eberly J H 2004 *Phys. Rev. Lett.* **93** 140404
[26] López C E, Romero G, Lastra F, Solano E and Retamal J C 2008 *Phys. Rev. Lett.* **101** 080503
[27] Reichman D R and Silbey R J 1996 *J. Chem. Phys.* **104** 1506
[28] Wang H, Thoss M and Miller W H 2001 *J. Chem. Phys.* **115** 2979
[29] Wang H and Thoss M 2008 *New J. Phys.* **10** 115005
[30] Itano W M 2001 Perspectives on the quantum Zeno paradox arXiv:quant-ph/0612187v1
[31] Facchi P and Pascazio S 2002 *Phys. Rev. Lett.* **89** 080401
[32] Lidar D A, Chuang I L and Whaley K B 1998 *Phys. Rev. Lett.* **81** 2594
[33] Shiokawa K and Lidar D A 2004 *Phys. Rev.* A **69** 030302
[34] Thilagam A 2009 *J. Phys.: Condens. Matter* **21** 045504
[35] Thilagam A 2009 *J. Phys. A: Math. Theor.* **42** 335301
[36] Wootters W K 1998 *Phys. Rev. Lett.* **80** 2245
[37] Meyer D A and Wallach N R 2002 *J. Maths. Phys.* **43** 4273